



Limits on the Dependence of the Fine-Structure Constant on Gravitational Potential from White-Dwarf Spectra

J. C. Berengut, V. V. Flambaum, A. Ong, and J. K. Webb

School of Physics, University of New South Wales, Sydney, New South Wales 2052, Australia

John D. Barrow

DAMTP, Centre for Mathematical Sciences, University of Cambridge, Cambridge CB3 0WA, United Kingdom

M. A. Barstow and S. P. Preval

Department of Physics and Astronomy, University of Leicester, University Road, Leicester LE1 7RH, United Kingdom

J. B. Holberg

Lunar and Planetary Laboratory, University of Arizona, Sonett Space Science Building, Tucson, Arizona 85721, USA

(Received 6 May 2013; published 3 July 2013)

We propose a new probe of the dependence of the fine-structure constant α on a strong gravitational field using metal lines in the spectra of white-dwarf stars. Comparison of laboratory spectra with far-UV astronomical spectra from the white-dwarf star G191-B2B recorded by the Hubble Space Telescope Imaging Spectrograph gives limits of $\Delta\alpha/\alpha = (4.2 \pm 1.6) \times 10^{-5}$ and $(-6.1 \pm 5.8) \times 10^{-5}$ from FeV and NiV spectra, respectively, at a dimensionless gravitational potential relative to Earth of $\Delta\phi \approx 5 \times 10^{-5}$. With better determinations of the laboratory wavelengths of the lines employed these results could be improved by up to 2 orders of magnitude.

DOI: [10.1103/PhysRevLett.111.010801](https://doi.org/10.1103/PhysRevLett.111.010801)

PACS numbers: 06.20.Jr, 31.15.am, 32.30.Jc, 97.20.Rp

Light scalar fields can appear very naturally in modern cosmological models and theories of high-energy physics, changing parameters of the standard model such as fundamental coupling constants and mass ratios. Like the gravitational charge, the scalar charge is purely additive, so near massive objects such as white dwarfs the effect of the scalar field can change. For objects that are not too relativistic, such as stars and planets, both the total mass and the total scalar charge are simply proportional to the number of nucleons in the object. However, different types of coupling between the scalar field and other fields can lead to an increase or decrease in scalar coupling strengths near gravitating massive bodies [1]. For small variations, the scalar field variation at distance r from such an object of mass M is proportional to the change in dimensionless gravitational potential $\phi = GM/rc^2$, and we express this proportionality by introducing the sensitivity parameter k_α [2]. Specifically, for changes in the fine-structure “constant” α , we write

$$\Delta\alpha/\alpha \equiv \frac{\alpha(r) - \alpha_0}{\alpha_0} \equiv k_\alpha \Delta\phi = k_\alpha \Delta\left(\frac{GM}{rc^2}\right).$$

This dependence can be seen explicitly in particular theories of varying α , such as those of Bekenstein [3] and Barrow-Sandvik-Magueijo [4], and their generalizations [5], where α can increase ($\Delta\alpha/\alpha > 0$) or decrease ($\Delta\alpha/\alpha < 0$) on approach to a massive object depending on the balance between electrostatic and magnetic energy in the ambient matter fields [1]. The most sensitive current

limits on k_α come from measurements of two Earth-bound clocks over the course of a year [2,6–12]. The sensitivity is entirely due to ellipticity in Earth’s orbit, which gives a 3% seasonal variation in the gravitational potential at Earth due to the Sun. The peak-to-trough sinusoidal change in the potential has magnitude $\Delta\phi = 3 \times 10^{-10}$. Each clock has a different sensitivity to α variation, and so $\Delta\alpha/\alpha$ can be measured and hence k_α extracted.

Because of the high precision of atomic clocks, k_α is determined very precisely despite the relatively small seasonal change in the gravitational potential. By contrast, we examine a “medium strength” field, where $\Delta\phi$ is 5 orders of magnitude larger than in the Earth-bound experiments, and the distance between the probe and the source is $\sim 10^4$ times smaller than 1 AU. This allows us to probe nonlinear coupling of $\Delta\alpha/\alpha$ on $\Delta\phi$, or the effects of a scalar charge Q which produces a Yukawa-like scalar field $\Phi = Qe^{-mr}/r$, where m is the (very small) mass of the scalar.

In this work we use the high-resolution far-UV spectrum of the nearby (≈ 45 pc [13]), hot hydrogen-rich (DA) white dwarf G191-B2B, recorded by the Hubble Space Telescope (HST) Imaging Spectrograph (STIS), which contains several hundred absorption lines identified as FeV and NiV transitions [14]. These iron and nickel ions reside in the atmosphere of the white dwarf and the observed features are formed in its outer layers, near the surface of white dwarf. Consequently, the ions experience the strong downward surface gravity of the star, $\log g = 7.53 \pm 0.09$, but are supported against this by the transfer

of momentum from high-energy photons, a process termed “radiative levitation” [15]. Here, $g = GM/R^2$ in cgs units, with $M_{\text{WD}} = 0.51M_{\odot}$ and $R_{\text{WD}} = 0.022R_{\odot}$ [14]. The gravitational potential for ions in the atmosphere of this white dwarf relative to the laboratory is $\Delta\phi \approx 5 \times 10^{-5}$.

To extract dependence on any α variation we first calculate the sensitivity coefficient for each line. As in previous work, we parametrize the sensitivity of the transition frequency to a variation in α from the laboratory value α_0 by the q coefficient, defined in terms of the line frequency ω by

$$q = \left. \frac{d\omega}{dx} \right|_{x=0}, \quad (1)$$

where $x \equiv (\alpha/\alpha_0)^2 - 1 \approx 2\Delta\alpha/\alpha$ is the fractional (small) change in α^2 . The frequencies of lines that are observed in the white-dwarf spectra are shifted from their laboratory values ω_0 due to the sum of Doppler and gravitational redshifts z and any potential gravitational α dependence near the white dwarf:

$$1 + z = \frac{\omega_0 + qx}{\omega}.$$

The relationship between the laboratory wavelengths and those observed near the white dwarf is

$$\frac{\Delta\lambda}{\lambda_0} = \frac{\lambda - \lambda_0}{\lambda_0} = z - Q_{\alpha} \frac{\Delta\alpha}{\alpha} (1 + z), \quad (2)$$

where $Q_{\alpha} = 2q/\omega_0$ is the relative sensitivity of the transition frequency to variation in α . In Fig. 1 we present a graph of $\Delta\lambda/\lambda$ vs Q_{α} for both FeV lines (blue circles) and NiV lines (red squares). The data used to generate these graphs can be found in [16].

To determine the sensitivity coefficients q for each line, we perform an *ab initio* calculation of the spectrum for $x = -0.01, 0.0, \text{ and } 0.01$, and then extract q using (1). The spectrum is calculated using the CI + MBPT method [17],

a combination of configuration-interaction (CI) and many-body perturbation theory (MBPT). Details of the implementation can be found in [18–20]. Here, we outline only the important points and defer details to a later work. The final q values are presented in [16].

For both FeV and NiV we start with a Dirac-Fock calculation in the V^N potential (i.e., the self-consistent field of all electrons) including the valence configuration $3d^n$ where $n = 4$ for FeV and $n = 6$ for NiV. In this procedure we simply scale the Dirac-Fock potential of the filled $3d^{10}$ shell by the number of valence electrons. We then form a B -spline basis by diagonalizing a set of splines over the self-consistent potential, which we use to form configurations with specified total angular momenta for our CI calculation. Configurations are formed by taking single and double excitations from the leading configurations $3d^n$, $3d^{n-1}4s$, and $3d^{n-1}4p$. In the case of FeV we use a B -spline basis of size $11spdf7g$ and include all single and double excitations from the leading configurations. The resulting energy levels are sufficiently close (within $\sim 2\%$) to the available data [21].

For NiV, the number of valence orbitals used for the CI calculation is markedly smaller. We include single-electron excitations to $12spdf$ and double excitations up to $5spdf$ from the leading configurations (a similar strategy was used for CrII in [22]). Results using all single and double excitations to $7s6pdf$ were consistent, although the final energies were not as good. MBPT corrections using a valence basis of $30spdfgh$ were then added to the CI calculations, which improve the overall agreement with the experimental values (again level energies are within $\sim 2\%$). Note that while the q values themselves do not change very much with the addition of MBPT corrections for either ion, the energy levels are much better and this helps with their identification.

The HST STIS spectrum utilized in this work is unique in coupling the highest signal-to-noise ratio so far achieved

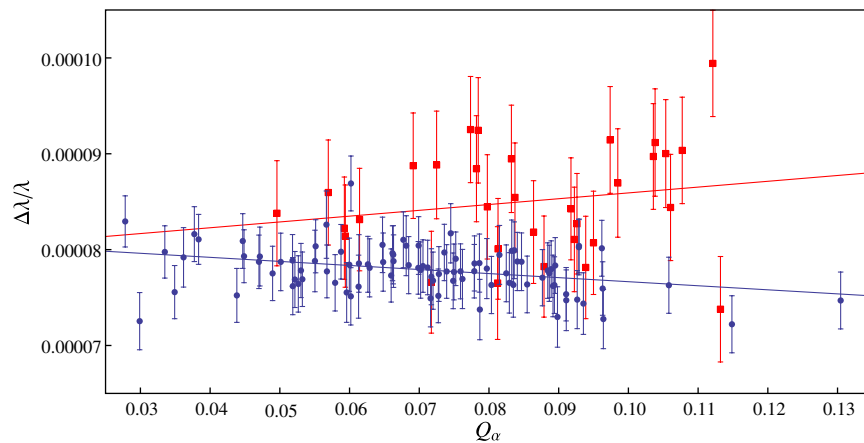


FIG. 1 (color online). $\Delta\lambda/\lambda$ vs Q_{α} for transitions in FeV (blue circles) and NiV (red squares). The slope of the lines gives $\Delta\alpha/\alpha = (4.2 \pm 1.6) \times 10^{-5}$ and $(-6.1 \pm 5.8) \times 10^{-5}$ for FeV and NiV, respectively. The slope seen in the NiV spectra is likely due to systematics present in the laboratory wavelength measurements rather than indicating a gravitational dependence of α .

for any white dwarf with the best spectral resolution and spectral coverage available with the instrument. The spectrum is constructed from a series of high-resolution (resolving power $R \approx 144000$) observations obtained with the E140H and E230H gratings as part of an extensive calibration program for the instrument, designed to provide flux calibration at the 1% level for all E140H and E230H primary and secondary echelle grating modes [23]. The detailed list of observations and their reduction, merging, and co-adding the components has been reported by [14].

In summary, the outcome of this work was two single continuous spectra spanning the wavelength ranges 1160–1680 Å and 1625–3145 Å for E140H and E230H, respectively. The signal-to-noise ratio is typically ≈ 50 but exceeds 100 at some wavelengths.

These spectra contain almost 1000 absorption features, mostly in the 1160–1680 Å region. Cross correlating their measured wavelengths with lines from the Kurucz [24] and University of Kentucky [25] lists yields 914 identifications. A large number of these correspond to FeV and NiV transitions. The detailed identification work has been reported by [14].

FeV.—Of the original 106 FeV transitions identified in the HST spectra, there are 96 for which there are good laboratory wavelengths (taken from [26]). Reference [26] estimates an uncertainty of 0.004 Å in their measurements, which dominates the errors for each value of $\Delta\lambda/\lambda$. From Fig. 1 we extract $\Delta\alpha/\alpha = (4.2 \pm 1.6) \times 10^{-5}$ (an apparent 2.6σ deviation from zero).

It is interesting to note that statistically the laboratory errors seem to be overestimated. Simply comparing the laboratory wavelengths with the HST data suggests that the actual error in the laboratory data is ~ 3 mÅ rather than the claimed 4 mÅ. An unweighted fit from Fig. 1 gives $\Delta\alpha/\alpha = (4.3 \pm 1.2) \times 10^{-5}$.

One potential source of systematic error is the calibration of the laboratory measurements or the astronomical data. Offset errors will not affect our result, since this

simply causes a change in the measured Doppler shift z . On the other hand, gain calibration errors—a linear mapping between the real and the measured λ —*could* cause a spurious detection of gravitational α dependence *if* there is also a correlation between Q_α and λ . If there is no correlation, then any gain error would not matter since the data points would be completely randomized on the Q_α axis.

In fact, such a correlation does exist. Energy levels of an ion that have a larger binding energy tend to spend more time closer to the nucleus, and therefore have larger relativistic effects. Therefore, higher energy transitions (smaller λ) will tend to have a larger difference in the relativistic effects between the upper and lower levels, and hence have larger q . The correlation between q and λ_0 is -0.45 for the FeV lines used (there is no evidence of nonlinear correlations). Therefore, gain shift in the laboratory measurements or the calibration of the HST spectrograph would be a possible source of error.

We can account for the potentially spurious detection of α variation that may occur by first removing any linear dependence of $\Delta\lambda/\lambda$ on λ (see Fig. 2). The line of best fit for FeV (blue) in Fig. 2 is $(\Delta\lambda/\lambda)_{\text{model}} = 7.79 \times 10^{-5} + 1.25 \times 10^{-8}(\lambda_0 - 1394 \text{ Å})$. Here, the first term [see Eq. (2)], $z_{\text{abs}} = 7.79 \times 10^{-5}$, is the average total redshift of the FeV lines. The fitted model values, $(\Delta\lambda/\lambda)_{\text{model}}$ as a function of λ_0 , are removed from the observed values of $\Delta\lambda/\lambda$ and we plot these against Q_α to obtain a new value of $\Delta\alpha/\alpha = (2.8 \pm 1.6) \times 10^{-5}$, consistent with zero at the 1.77σ level (although again we note that if we reduce the assumed laboratory errors to the level suggested by the data, the error in $\Delta\alpha/\alpha$ is of order 1.2×10^{-5}). Note that while we have removed the potential systematic due to calibration error, we have also potentially lost a real signal of $\Delta\alpha/\alpha$. Ultimately, well-calibrated laboratory and astronomical data will remove the need for this procedure and boost the sensitivity of this method.

NiV.—Laboratory data for NiV are provided by [27], who estimate their uncertainty as ~ 1 mÅ [28]. In fact,

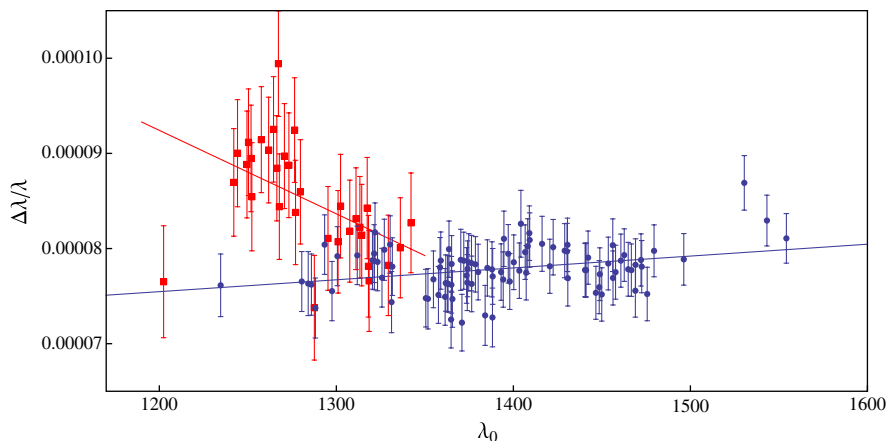


FIG. 2 (color online). $\Delta\lambda/\lambda$ vs λ_0 for transitions in FeV (blue circles) and NiV (red squares). The correlation seen here could be due to calibration systematics, or gravitational dependence of α since Q_α and λ_0 are (anti)correlated.

based on comparison with the HST data, this seems likely to be an underestimate. In Fig. 1 we use an assumed laboratory error of 7 mÅ, which leads to a more realistic distribution of residuals. Calculations for NiV are also more difficult than for FeV, and in several cases potentially useful transitions were not used because the levels could not be uniquely identified in our calculations. In other cases the original laboratory data were blended (which, aside from being flagged in [27], lead to obvious $>3\sigma$ outliers in Fig. 1). In total, 32 NiV transitions were used out of the 44 identified in HST spectra. The slope of the line in Fig. 1 gives a value of $\Delta\alpha/\alpha = (-6.1 \pm 5.8) \times 10^{-5}$, consistent with zero at the 1.05σ level.

As we did for FeV, we removed any potential gain-shift systematic by subtracting the linear dependence of $\Delta\lambda/\lambda$ on λ : $(\Delta\lambda/\lambda)_{\text{model}} = 8.51 \times 10^{-5} - 8.77 \times 10^{-8}(\lambda_0 - 1283 \text{ \AA})$ (red line in Fig. 2). Note that for NiV the slope is in the opposite direction to that of FeV and is much larger (that is, $\Delta\lambda/\lambda$ tends to be smaller in transitions with longer wavelengths). Plotting $\Delta\lambda/\lambda - (\Delta\lambda/\lambda)_{\text{model}}$ against Q_α gives a line of best fit $\Delta\alpha/\alpha = (-2.5 \pm 5.8) \times 10^{-5}$, within 0.4σ of zero.

The two values for $\Delta\alpha/\alpha$ that we have obtained (shown in Fig. 1) seem inconsistent: the FeV data indicate $\Delta\alpha/\alpha > 0$, while the NiV data indicate $\Delta\alpha/\alpha < 0$. Formally, the weighted mean of the two values is $\Delta\alpha/\alpha = (3.5 \pm 1.5) \times 10^{-5}$, which is dominated by the FeV result and consistent with the NiV result at 1.6σ . Figure 2 suggests that the slope seen in the NiV data is a systematic present in the laboratory wavelength measurements, rather than indicating a gravitational dependence of α . Indeed, removing this potential systematic as described above brings both sets of data into agreement within 1σ .

The linear dependence of α on gravitational potential derived from the FeV measurement is $k_\alpha = 0.7 \pm 0.3$, which is much weaker than the limit derived from atomic clocks, where the best current limit is $k_\alpha = (-5.5 \pm 5.2) \times 10^{-7}$ [12]. The aim of this work, however, is not to find k_α , but to find the dependence of α on gravitational potential mediated by a light scalar field. The white-dwarf result probes a “medium field” limit, where the change in dimensionless gravitational potential is 5 orders of magnitude larger than probed using clocks, and the distance between the source and the probe is 4 orders of magnitude smaller. The limit on $\Delta\alpha/\alpha$ derived from analysis of white-dwarf spectra may be more sensitive to nonlinear coupling of scalar fields to α , or α dependence due to a Yukawa-like scalar field with non-zero scalar mass.

We can compare the limits on the change in α measured in this system with the application of the many-multiplet method to a quasar absorption system [29,30], which typically are at the $\Delta\alpha/\alpha \sim O(10^{-5})$ level. Firstly, we are using ~ 100 lines, rather than ~ 10 , per system used in quasar studies. This gives us a statistical advantage over the

quasar studies. Secondly, the q values are much larger here since we are using more highly ionized species. Taken together, this study should have more than an order-of-magnitude higher sensitivity per system than the quasar studies, and we should be reaching statistical accuracies below 10^{-6} . Unfortunately, at present we are limited by relatively poor laboratory wavelengths. In the future, this limitation may be circumvented by comparing two white dwarfs (or other stars) with different surface gravities. New measurements of the FeV and NiV spectra could improve the limit by up to 2 orders of magnitude.

It is interesting to note that the gravitational redshift, $z = \Delta\phi \approx 5 \times 10^{-5}$, is the dominant contribution to the average total redshift, $z_{\text{abs}} = 7.78 \times 10^{-5}$ for FeV and 8.47×10^{-5} for NiV. With improvement in laboratory wavelengths, this system should also be able to provide a test of the equivalence principle of general relativity in a “medium strength” field with higher accuracy and provide constraints on other variations of traditional “constants” driven by scalar fields in the universe [1,31,32].

-
- [1] J. Magueijo, J. D. Barrow, and H. Sandvik, *Phys. Lett. B* **549**, 284 (2002).
 - [2] V. V. Flambaum and E. V. Shuryak, *AIP Conf. Proc.* **995**, 1 (2008).
 - [3] J. D. Bekenstein, *Phys. Rev. D* **25**, 1527 (1982).
 - [4] H. B. Sandvik, J. D. Barrow, and J. Magueijo, *Phys. Rev. Lett.* **88**, 031302 (2002); J. D. Barrow, H. B. Sandvik, and J. Magueijo, *Phys. Rev. D* **65**, 063504 (2002).
 - [5] J. D. Barrow and S. Z. W. Lip, *Phys. Rev. D* **85**, 023514 (2012).
 - [6] A. Bauch and S. Weyers, *Phys. Rev. D* **65**, 081101 (2002).
 - [7] S. J. Ferrell, A. Cingöz, A. Lapiere, A.-T. Nguyen, N. Leefler, D. Budker, V. V. Flambaum, S. K. Lamoreaux, and J. R. Torgerson, *Phys. Rev. A* **76**, 062104 (2007).
 - [8] T. M. Fortier, N. Ashby, J. C. Bergquist, M. J. Delaney, S. A. Diddams, T. P. Heavner, L. Hollberg, W. M. Itano, S. R. Jefferts, K. Kim, F. Levi, L. Lorini, W. H. Oskay, T. E. Parker, J. Shirley, and J. E. Stalnaker, *Phys. Rev. Lett.* **98**, 070801 (2007).
 - [9] S. Blatt, A. D. Ludlow, G. K. Campbell, J. W. Thomsen, T. Zelevinsky, M. M. Boyd, J. Ye, X. Baillard, M. Fouche, R. Le Targat, A. Brusch, P. Lemonde, M. Takamoto, F.-L. Hong, H. Katori, and V. V. Flambaum, *Phys. Rev. Lett.* **100**, 140801 (2008).
 - [10] J. D. Barrow and D. J. Shaw, *Phys. Rev. D* **78**, 067304 (2008).
 - [11] J. Guéna, M. Abgrall, D. Rovera, P. Rosenbusch, M. E. Tobar, P. Laurent, A. Clairon, and S. Bize, *Phys. Rev. Lett.* **109**, 080801 (2012).
 - [12] N. Leefler, C. T. M. Weber, A. Cingöz, J. R. Torgerson, and D. Budker, *arXiv:1304.6940*.
 - [13] N. Reid and G. Wegner, *Astrophys. J.* **335**, 953 (1988).
 - [14] S. P. Preval, M. A. Barstow, J. B. Holberg, and N. J. Dickinson (to be published).

- [15] P. Chayer, S. Vennes, A.K. Pradhan, P. Thejll, A. Beauchamp, G. Fontaine, and F. Wesemael, *Astrophys. J.* **454**, 429 (1995).
- [16] See Supplemental Material at <http://link.aps.org/supplemental/10.1103/PhysRevLett.111.010801> for tables of laboratory and observed wavelengths and calculated q values for lines used in this analysis.
- [17] V.A. Dzuba, V.V. Flambaum, and M.G. Kozlov, *Phys. Rev. A* **54**, 3948 (1996).
- [18] J.C. Berengut, V.V. Flambaum, and M.G. Kozlov, *Phys. Rev. A* **72**, 044501 (2005).
- [19] J.C. Berengut, V.V. Flambaum, and M.G. Kozlov, *Phys. Rev. A* **73**, 012504 (2006).
- [20] J.C. Berengut, V.V. Flambaum, and M.G. Kozlov, *J. Phys. B* **41**, 235702 (2008).
- [21] J. Sugar and C. Corliss, *J. Phys. Chem. Ref. Data* **14**, Suppl. No. 2, 1 (1985).
- [22] J.C. Berengut, *Phys. Rev. A* **84**, 052520 (2011).
- [23] J.B. Holberg, M.A. Barstow, I. Hubeny, M.S. Sahu, F.C. Bruhweiler, and W.B. Landsman, *ASP Conf. Ser.* **291**, 383 (2003).
- [24] R.L. Kurucz, *Can. J. Phys.* **89**, 417 (2011); <http://kurucz.harvard.edu>.
- [25] P. van Hoof, <http://www.pa.uky.edu/~peter/newpage>.
- [26] J.O. Ekberg, *Phys. Scr.* **12**, 42 (1975).
- [27] A.J.J. Raassen and Th.A.M. van Kleef, *Physica (Amsterdam)* **85C**, 180 (1977).
- [28] A.J.J. Raassen, Th.A.M. van Kleef, and B.C. Metsch, *Physica (Amsterdam)* **84C**, 133 (1976).
- [29] V.A. Dzuba, V.V. Flambaum, and J.K. Webb, *Phys. Rev. Lett.* **82**, 888 (1999).
- [30] J.K. Webb, V.V. Flambaum, C.W. Churchill, M.J. Drinkwater, and J.D. Barrow, *Phys. Rev. Lett.* **82**, 884 (1999).
- [31] T. Dent, *Phys. Rev. Lett.* **101**, 041102 (2008).
- [32] J.C. Berengut and V.V. Flambaum, *Europhys. Lett.* **97**, 20006 (2012).